Effect of Al 2 O 3 thickness and oxidant precursors on the interface composition and contamination in Al 2 O 3 /GaN structures

Tarek Spelta, Eugénie Martinez, Marc Veillerot, Pedro Fernandes Paes Pinto Rocha, Laura Vauche, Bassem Salem, Bérangère Hyot

Effect of Al_2O_3 thickness and oxidant precursors on the interface composition and contamination in Al_2O_3/GaN structures

Tarek Spelta[1]*, Eugénie Martinez[1], Marc Veillerot[1], Pedro Fernandes Paes Pinto Rocha[1], Laura Vauche[1], Salem Bassem[2], Bérangère Hyot[1],

[1]*Univ. Grenoble Alpes, CEA, Leti, F-38000 Grenoble, France*

[2]*Univ. Grenoble Alpes, CNRS, LTM, F-38000 Grenoble, France*

**e-mail contact: tarek.spelta@cea.fr*

In this paper, we discuss the combined characterization by time-of-flight secondary ion mass spectrometry (ToF-SIMS) and hard x-ray photoelectron spectroscopy (HAXPES) of the Al_2O_3/GaN interface for the next generation of MOS-gate GaN-based devices. The final properties of these devices strongly depend on the quality of this critical interface. Results highlight that gallium oxidation at this interface is enhanced when increasing atomic layer deposited (ALD) Al_2O_3 thicknesses from 3 nm up to 20 nm. Moreover, we highlight how Al_2O_3 (O_3/H_2O)/GaN structures reduce the oxidation of gallium compared to Al_2O_3 (H_2O) structures, where O_3 and H_2O are the oxygen precursors for ALD of Al_2O_3. In addition, through ToF-SIMS measurements we show the effect in terms of contaminants (hydrogen, carbon, halide) at the Al_2O_3/GaN interface depending on the oxygen precursor used.

Keywords: HEMT, GaN, oxidation, ToF-SIMS, HAXPES

I. INTRODUCTION

The incessant growth of electricity consumption, in an era in which we are heading towards fossil fuel replacement and a better management of energy use, requires electronic devices that can meet these needs [1]. For power electronics, silicon-based devices such as insulated gate bipolar transistors (IGBTs) or metal oxide semiconductor field effect transistors (MOSFETs) have played a

fundamental role in controlling the electric current and therefore the electric power consumption [2], [3]. While silicon-based devices are reaching their operational limits, power electronics devices research has turned towards III-N materials. In particular, gallium nitride (GaN) is considered as an excellent candidate for the next generation devices in the field. Compared to Si, GaN shows a higher breakdown field and a higher bandgap thus allowing to design devices working at higher voltages [4]. Moreover, GaN devices can produce lower losses in R_{on} at high voltages and temperatures. Hence, they can be operated at higher frequencies for example in RF applications [5]**.** In addition to the different physical properties mentioned above indicating the superior aspects of GaN with respect to Si, the greater performances of the GaN transistors lie in their particular AlGaN/GaN structure. The junction of these two alloys promotes greater electron mobility due to the two dimensional electron gas (2-DEG) located at this interface [6].

However, there are still some aspects to clarify in order to optimize the final performances of GaN high electron mobility transistors (HEMTs). The presence of a 2-DEG at the AlGaN/GaN interface implies a passage of perennial current between the source and drain, yielding to "normally ON" devices. For safety reasons, especially for power applications, several technologies are implemented to build normally OFF structures [7] allowing reduced electrical consumption. Among the various options, the fully recessed gate MOS-channel HEMT (MOSc-HEMT) is a promising solution [8] (see figure 1). In this type of structures, a full removal of AlGaN layer and partial etching of GaN is required. The etching process damages the GaN interface and, for this reason, before depositing the Al_2O_3 dielectric via atomic layer deposition (ALD), the GaN surface is subject to various wet chemical treatments to reduce surface contamination, such as carbon and etching chemical residues [9]. This surface treatment is also crucial to remove the native gallium oxide and to reduce the GaN roughness before depositing the Al_2O_3 [10].

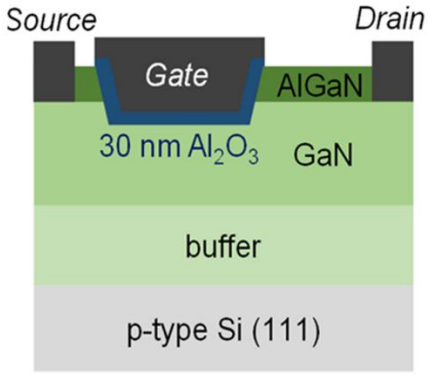

Figure 1. Scheme of the GaN MISHEMT structure.

The performances of these MISHEMT GaN structures are related to the quality of the buried Al_2O_3/GaN critical interface, which strongly relies on the GaN etching and cleaning steps. The properties of this interface also depends on the dielectric characteristics, related to the deposition method and thickness. In this paper, we will study the quality of the Al_2O_3/GaN interface in terms of gallium surface oxidation and contamination when varying the Al_2O_3 thickness and oxidant precursors. This gallium oxidation is particularly deleterious for the final performances of the devices since it shifts the V_{th}, thus leading to a normally-On device [11]. Both ToF-SIMS and HAXPES measurements are carried out to provide complementary information, regarding the composition with high depth resolution and the chemical bonds up to 20 nm depth, respectively.

II. EXPERIMENTAL DETAILS

GaN n-doped was grown on Si wafers using metal organic chemical vapor deposition (MOCVD) on top of several AlGaN/GaN buffer layers. To mimic the MISHEMT fabrication, an etching step was performed using inductively couple plasma reactive ion etching (ICP-RIE) with a Cl based chemistry. The GaN surface was then treated with a chemical wet treatment including hydrofluoric acid (HF) as a last step, known to be efficient for gallium oxide removal [12]. The Al_2O_3 was then deposited by atomic layer deposition (ALD) at 300°C using Trimethylaluminium (TMA) and water (H_2O) as precursors, on etched GaN surfaces with increasing Al_2O_3 thicknesses of 3, 10 and 20 nm (samples

A1, B1, C1). In order to study the effect of the oxidant precursor, we have tested another dielectric, a bi-layer composed of a first 5-nm thick Al_2O_3 layer deposited using H_2O covered by an Al_2O_3 layer deposited using O_3 as precursor, with thicknesses varying from 5, 10 and 15 nm, yielding to overall thicknesses of 10, 15 and 20 nm (D1, E1, F1). The thickness of the different aluminas were determined by ellipsometry with an error bar of ± 1 nm with the exception of the sample A1 where the the error bar is ± 1.2 nm. All the details about the samples fabrication are summarized in Table 1. Two additional samples were used as references: an as-epitaxied GaN on Si (without etching and HF wet treatments) and a bulk Ga_2O_3 sample from Novel Crystal Technology, Inc.

Table 1. Samples description

Sample name	A1	B1	C1	D1	E1	F1
ALD Al_2O_3 thickness	3 nm	10 nm	20 nm	10 nm	15 nm	20 nm
Precursors	H_2O	H_2O	H_2O	O_3/H_2O	O_3/H_2O	O_3/H_2O
Etched GaN	Yes					
Wet treatment	HF					

HAXPES measurements were made with a Quantes from ULVAC-PHI equipped with two monochromatized and confocal Al Kα (hν=1486.7 eV) and Cr Kα (hν=5.415 keV) X-ray sources. Beam sizes of 100 µm and 200 µm were respectively used for each sources. The measurements were carried out with a pass energy of 23 and 55 eV, leading to energy resolutions of 0.6 and 0.9 eV for the Al and Cr sources respectively. With the Cr Kα source, the photoelectrons were collected with a take-off angle (TOA) θ of 90° and considering the variety of samples comprising different Al_2O_3 thicknesses, we estimated an average value of the Ga 2p inelastic mean free path taking into account the aluminum thickness at each sample. The inelastic mean free path values in pure GaN (6.1 nm) and pure Al_2O_3 (8.1 nm) derive from the algorithm of Tanuma *et. al* [13]. The equation below estimates the averaged inelastic mean free path as the thickness of the alumina varies:

$$\lambda_{Ga\ 2p}^{average} = \frac{Al_2O_3\ thickness}{GaN\ escape\ depth} * \lambda_{Ga\ 2p}^{Al_2O_3} + \frac{GaN\ escape\ depth - Al_2O_3\ thickness}{GaN\ escape\ depth} * \lambda_{Ga\ 2p}^{GaN}$$

It can be seen that the greater the thickness of the aluminum and the greater the inelastic mean free path, which will tend to have a value close to that in the Al_2O_3 matrix. A dual-beam system combining electrons and argon ions was used to compensate charges. All the spectra were decomposed with pseudo-Voigt functions after Shirley background subtraction using Casa XPS v2.3 software.

The great improvement of HAXPES with respect to XPS is the higher photon energy offering the possibility to collect photoelectrons with higher kinetic energy coming from deeper inside samples, in particular from critical buried interfaces. The Al_2O_3/GaN interface characterization by XPS with an Al Kα source is usually carried out by analyzing the Ga 3d core level to get information about the gallium chemical environment [11] but this cannot be totally achieved when working with a higher photon energy because of the photoelectron cross sections decrease [18]. As a consequence, when working with a Cr Kα source, the Ga 2p core level is more suitable for the analysis of the Ga oxidation because the cross-section is higher than the Ga 3d one [19]. Thus, in our case, the peaks analyzed to better understand this interface are the following: Ga 2p, N 1s, Al 1s, O 1s.

In order to properly extract some chemical information from the Ga 2p core level, which is quite symmetric and thus difficult to decompose, we have carried out a methodological work to check the binding energy gap between the gallium nitride (Ga-N bonds) and gallium oxide (Ga-O bonds) environments. First, XPS measurements with the Al Kα source were performed on the GaN and Ga2O3 reference samples. The Ga 2p core-level spectra were calibrated with respect to the C 1s peak (284.8 eV) and the energy shift between the two spectra was found to be +0.7 eV (see figure 2a). Then HAXPES measurements were also carried out with the Cr Kα source (see figure 2b). Given the low intensity of the C 1s peak, the binding energy scale was calibrated according to the N 1s peak position (397 eV) as measured with the Al Kα source for the GaN and to the O 1s core level (530.7 eV)

for the Ga_2O_3. From figure 2b, a chemical shift equal to +0.8 eV was measured, in agreement with the observations made with the Al Kα source.

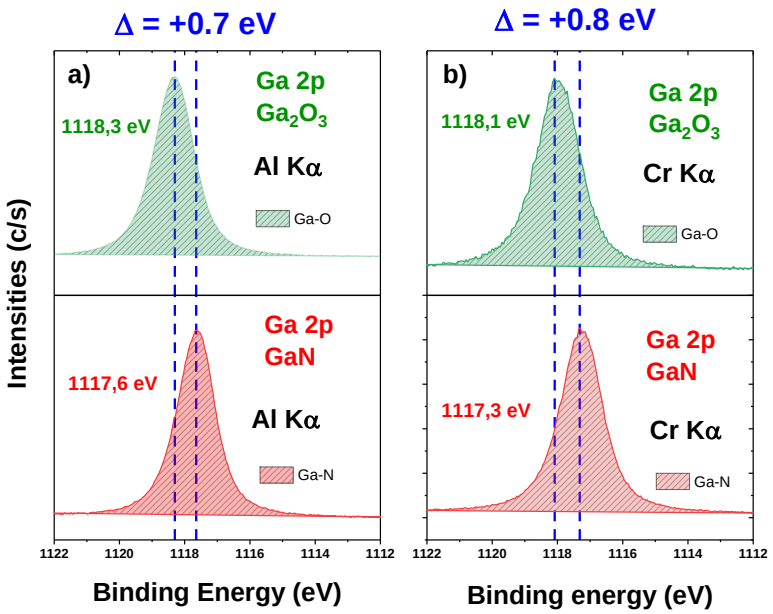

Figure 2. Ga 2p core level spectra measured on the GaN and Ga_2O_3 samples a) with the Al Kα source, b) with the Cr Kα source.

For the rest of the paper, the Ga 2p peak was thus decomposed using two contributions related to Ga-N and Ga-O bonds. From the previous measurements, the energy shift between these components was fixed at 0.7 eV, as also reported in the literature [14]–[16]. In addition, the full width at half maximum (FWHM) of the components was fixed at a maximum of $1.5\ eV$ for the Ga-N contribution and 2.5 eV for the Ga-O contribution. The components were fitted with a combination of Gaussian (80%) and Lorentzian (20%) for Ga-N and only a Gaussian (100%) for Ga-O. All the experimental parameters used to decompose the Ga 2p core level are summarized in Table 2.

Table 2. HAXPES parameters used for the decomposition of Ga 2p in Al_2O_3/GaN structures

	Ga-N	Ga-O
FWHM (eV)	1.5	2.5
Shift (eV)	ref	+0.7
G/L (%)	80/20	100/0

ToF-SIMS analyses were carried out using a dual beam TOF 5 instrument from IONTOF Gmbh. The depth profiles were obtained using a Cs^+ sputter beam at 500 eV and 25 nA and a Bi_3^+ analysis beam at 15 kV and 0.3 pA. Both ions guns were operated with an incidence angle of 45° with respect to the sample surface. A sputter area of 300 μm^2 and an analysis area of 80 µm² were used. To investigate gallium oxidation, the analysis was conducted in the secondary ions (SI) positive MCs_2^+ mode, allowing a reliable depth profiling of the main compositional elements such as Al, Ga, N, O. The motivation of the MCs_2^+ modality is due to the matrix effects that occur when analyzing structures with different composition. As reported in various scientific papers, the ionization efficiency can vary significantly with the variation of the interface studied and therefore can mislead about the real composition of the elements studied. [15]–[17]. The profiles were all normalized point by point using the Cs_2^+ signal. The aim here to use MCs_2^+ approach is to avoid at best matrix effects during our depth profiles. For the analysis of contaminants, the negative mode was used to follow the main elements such as H, C, F and Cl present on these structures. The profiles measured in negative mode were all normalized with respect to the stabilized bulk GaN^- signal of the GaN matrix. This permitted us to have a stable calibration signal considering that all the GaN matrix have the same bulk thickness and chemical composition. The interfaces of our Al_2O_3/GaN depth profiling were determined upon reaching 50% of the $GaCs_2^+$ and GaN^- signals strength with respect to the signal present in the bulk. It is an arbitrary criterion used to define the interfaces of our ToF-SIMS analyzes for comparison purposes. For both modes of depth profiling, the depth scale was calibrated according to the thickness of the Al_2O_3 layer known with an uncertainty of ±0.9 nm, as controlled by TEM for the 10 nm-thick alumina layer.

III. RESULTS AND DISCUSSION

We investigate the Al_2O_3/GaN interface by combining ToF-SIMS and HAXPES measurements in order to obtain the chemical composition with high depth resolution and to investigate the gallium oxidation at this buried interface with an increased depth sensitivity.

III.1 Effect of alumina thickness and oxidant precursor on GaN oxidation

HAXPES measurements were performed on the Al_2O_3/GaN samples with increasing Al_2O_3 thicknesses while using only H_2O (x=3, 10 and 20 nm) and both O_3 and H_2O (x=10, 15 and 20 nm) as oxidant precursors (see figure 3). Our purpose is here to evaluate the effect of the Al_2O_3 thickness on the GaN oxidation, as well as to see if the precursors used for the alumina deposition have some influence on this oxidation.

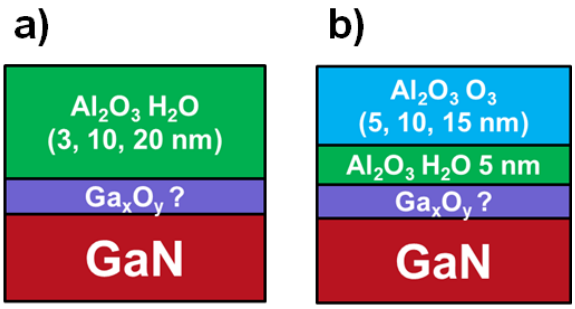

Figure 3. Al_2O_3/GaN structures a) with H_2O precursor, b) with O_3/H_2O precursors.

A detailed analysis of the Ga 2p peaks was done to extract both the Ga-O and Ga-N contributions, as explained in section II. An example of such decomposition is presented in figure 4a. Then, the gallium oxidation at the interface is estimated, in percentage, from the area ratio between the Ga-O component and the total area of the Ga 2p peak (sum of the Ga-O and Ga-N area), according to the following equation:

$$Ga-O\ (\%) = \frac{Area^{Ga-O}}{Area^{Ga-O} + Area^{Ga-N}} * 100$$

The results obtained for the different samples are shown in figure 4b. HAXPES measurements were all made with TOA of 90 ° in order to maximize the depth sensitivity. These results show that both the thickness and the oxidant precursor used to deposit the alumina, change the GaN oxidation level. First, the thicker the alumina layer, the more oxidized is the Al_2O_3/GaN interface. Second, the use of two precursors (O_3/H_2O) allows to significantly decrease the GaN oxidation compared to the use of H_2O. However, we denote that depending on the precursor employed, oxidation does not evolve in the same way. Samples with the bi-layered alumina (O_3/H_2O) tend to saturate towards a limited oxidation percentage (~18 %) while a clear increase of this oxidation percentage is observed on the Al_2O_3 H_2O samples. The error bars about the oxidation of the Ga 2p core level on the different samples were determined by averaging different background regions of the Ga 2p peak with a final estimate of 15% error.

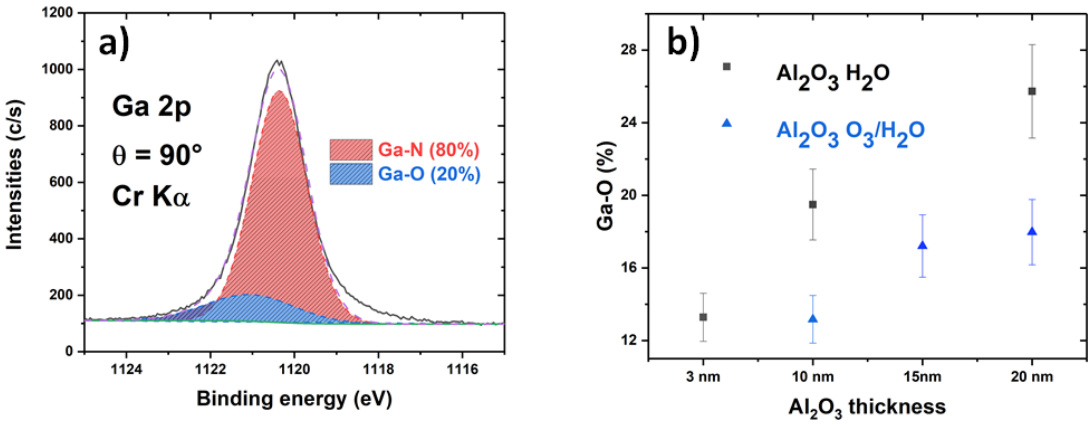

Figure 4. a) HAXPES Ga 2p spectrum measured for the 10 nm-thick Al_2O_3(H_2O)/etched GaN stack and b) Ga 2p oxidation measured versus Al_2O_3 thickness and oxidant precursor.

Complementary ToF-SIMS measurements were performed to observe the evolution of the oxygen profiles with increasing Al_2O_3 thickness. The profiles measured for the 10 nm-thick Al_2O_3 (full H_2O)/etched GaN (A1) are plotted in figure 5. The interface between the Al_2O_3 and the GaN layer (dashed line) is located when reaching 50 % of the maximum $^{69}GaCs_2^+$ profile intensity. This is of course an arbitrary criterion only used here with the purpose of comparing samples.

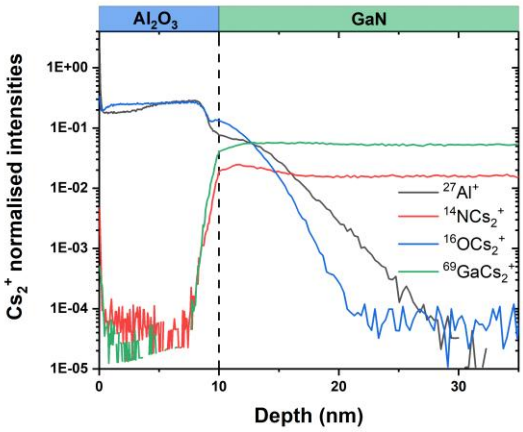

Figure 5. ToF-SIMS depth profile of 10 nm-thick Al_2O_3 (H_2O)/etched nGaN.

We now plot the $^{16}OCs_2^+$ profiles obtained for the full H_2O Al_2O_3/GaN samples (A1, B1, C1) and the O_3/H_2O Al_2O_3/GaN samples (D1, E1, F1) on figure 6a and 6b, respectively.

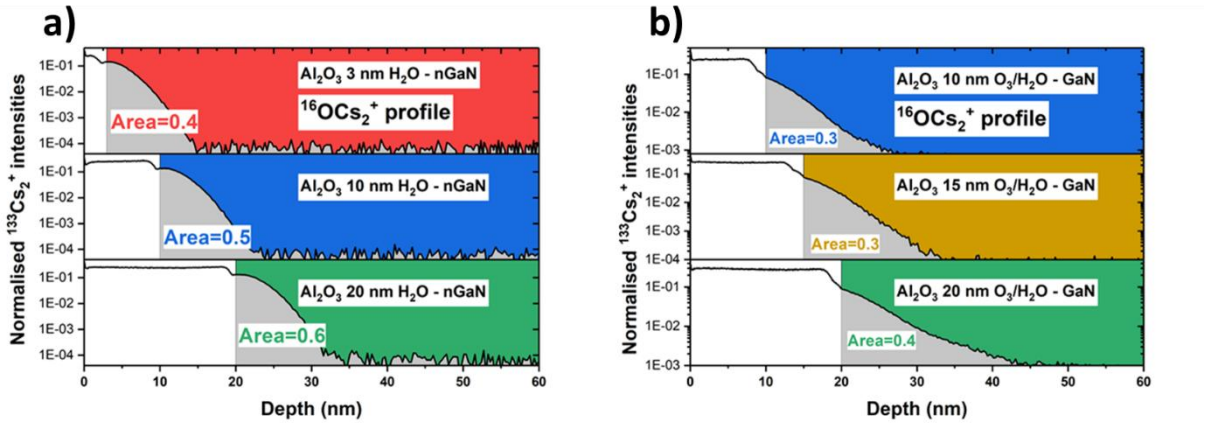

Figure 6. ToF-SIMS depth profiles of the a) full H_2O Al_2O_3(10 nm)/GaN stacks (A1, B1, C1) and b) O_3/H_2O Al_2O_3(10 nm)/GaN stacks (D1, E1, F1).

The integrated area (expressed in normalized intensity x nm) under the $^{16}OCs_2^+$ profiles starting from the interface (50 % of the $^{69}GaCs_2^+$ profile) until reaching the minimum intensity gives an estimate of the oxygen presence at the Al_2O_3/GaN interface. For the full H_2O Al_2O_3/GaN samples (A1, B1, C1), the areas are of 0.44 ± 0.03, 0.51 ± 0.05 and 0.58 ± 0.03 and for the O_3/H_2O Al_2O_3/GaN samples (D1, E1, F1), the areas are of 0.33 ± 0.03, 0.28 ± 0.02 and 0.44 ± 0.05. They were determined by taking

multiple measurements of the area under the aforementioned profile at different depths. These results are consistent with the previous HAXPES estimation of the gallium oxidation level. As such, they confirm an increase in the oxygen presence with increasing Al_2O_3 thickness and a slightly higher oxidation level when using only H_2O as the oxidant precursor instead of both O_3/H_2O.

III.2 Effect of alumina precursors on the Al_2O_3/GaN interface contamination

In addition to the effect on gallium oxidation observed with the combined ToF-SIMS and HAXPES approach highlighted in figure 4, 5 and 6, we show that depending on the precursor chosen to deposit Al_2O_3, the trace chemical composition at the interface changes. The information on the chemical presence of certain elements such as C, H, Cl, and F was obtained by ToF-SIMS analysis on samples B1, C1, D1, F1. The purpose of this comparison is to examine the chemical effect of the precursors on the Al_2O_3-GaN interface for the same thickness of deposited alumina (10 and 20 nm). In order to have a sufficient ionic efficiency, the ToF SIMS analyses for the detection of contaminants and impurities mentioned above were carried out with secondary ions of negative polarity. This allowed to have a greater sensitivity in obtaining the depth profiles. The dashed lines express the interfaces and they have been determined in the same manner as previously explained.

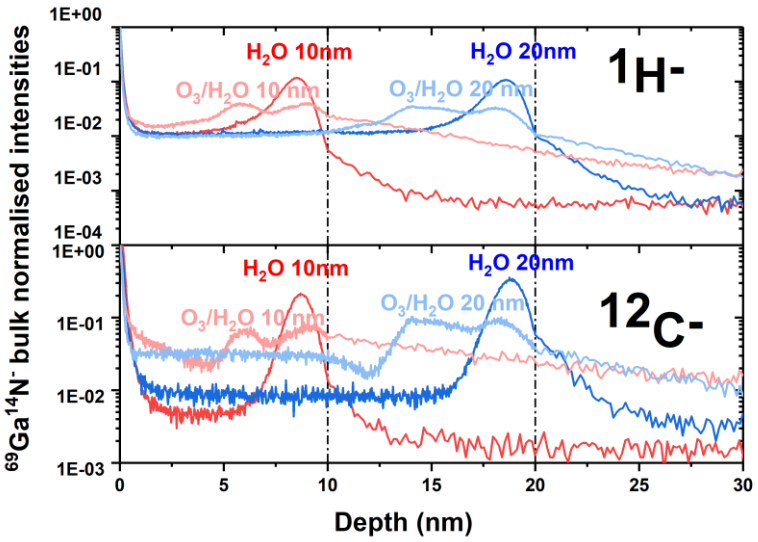

Figure 7. ToF-SIMS depth profiles of $^{12}C^-$ and $^1H^-$ into the samples B1, C1, D1, F1

From figure 7, it can be seen how through the TOF-SIMS characterization, we show the difference in structures between the two aluminas since on the O_3/H_2O aluminas, we denote the presence of two peaks which indicate the borders between the Al_2O_3 layers with O_3 and H_2O precursors. The other alumina with only one precursor exhibits only one peak, which therefore indicates a different type of structure. In addition, It can be seen how the Al_2O_3 (O_3/H_2O) structures allow to reduce the presence of carbon and hydrogen at the Al_2O_3/GaN interface. We assume that the hydroxyl groups (-OH) in the oxides can be reduced using O_3 as a precursor [20], [21]. As reported by Kubo *et. al* the combined use of H_2O and O_3 allows to reduce the presence of C and H in the alumina oxides deposited by ALD [22]. Indeed, in the research paper of Kubo *et. al*, it is mentioned that the introduction of the H_2O precursor after the introduction of trimethylaluminum (TMA) leads to chemical reactions such as: $-CH_3 + H_2O \rightarrow -OH + CH_4$ thus obtaining a surface with hydroxyl bonds -OH. Instead, using the O_3 precursor in the ALD process, the following reaction is obtained: $-6CH_3 + 2O_3 \rightarrow -6O + 3C_2H_6$. We therefore obtain a reduction of the hydroxyl bonds -OH with the O_3 precursor but at the same time we increase the presence of carbon oxides [23]. Hence, in order to reduce both C and H, it is necessary to combine the use of the H_2O and O_3 precursors, more precisely, by first introducing the H_2O precursor and then the O_3 precursor. The combined use of these two precursors will cut the O-H chemical bonds and prevent the formation of hydroxyl -OH bonds on the surface. In addition, we do observe a longer trail into the GaN matrix for ^{1}H and ^{12}C in the case of O_3/H_2O precursors. This phenomenon could be explained by a higher roughness due to the difference in precursors used to deposit the alumina, which therefore modify the typology of the alumina and consequently modifying the morphology of the surface. Additional measurements using technique such as Atomic Force Microscopy would be useful to confirm this assumption.

Conversely, we observe that the use of O_3/H_2O structures promotes the presence of chlorine and fluorine at the interface (see figure 8).

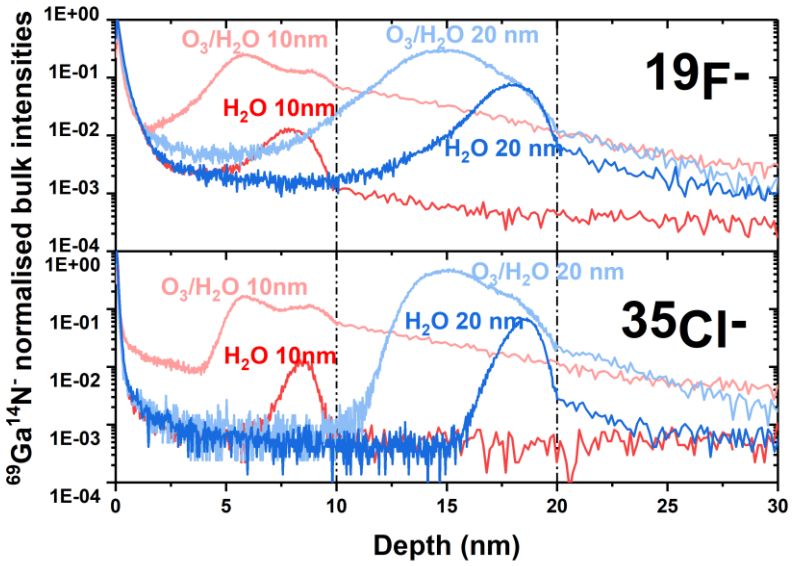

Figure 8. ToF-SIMS depth profiles of $^{19}F^-$ and $^{35}Cl^-$ into the samples B1, C1, D1, F1

The presence of these elements probably comes from the etching process in which a chemical process based on chlorine is used and the wet cleaning based on HF [24]. Consequently, we assume that the combination of O_3/H_2O precursors promotes the presence of chemical elements linked to the etching and cleaning processes at the interface compared to H_2O structures.

IV. CONCLUSION

The interface quality of the buried Al_2O_3/GaN interface of MISHEMT GaN structures is crucial to preserve their electrical performances. We investigated the gallium oxidation for Al_2O_3/GaN stacks while increasing the Al_2O_3 thickness and changing the oxidant precursors. Our approach relying on the use of two complementary techniques, on one hand HAXPES, and on the other hand, ToF-SIMS was found to be very efficient to reveal the actual level of oxidation of such Al_2O_3/GaN buried interface. In addition, for HAXPES, a methodological approach was set considering spectra from references for increasing the reliability of the decomposition of the Ga 2p peak. The interfacial gallium oxidation is extracted from a detailed analysis of this core level. The enhanced depth sensitivity compared to XPS allows to investigate accurately such an oxidation with Al_2O_3 thicknesses

varying from 3 to 20 nm. Applied to experimental layers designed for setting the technological paths, the results highlight that the thicker the alumina layer, the more oxidized is the gallium at the buried Al_2O_3/GaN interface. HAXPES is thus here of real interest to probe an Al_2O_3/GaN interface as close as possible of the real one which is buried under a 30 nm-thick Al_2O_3 layer in the MISHEMT GaN structures. Moreover, the use of two precursors (O_3 and H_2O) was shown to be useful to reduce the gallium oxidation compared to use of only H_2O. These results are consistent with the ToF-SIMS oxygen profiles showing an increase oxygen presence with increasing Al_2O_3 thickness and for full H_2O Al_2O_3 compared to O_3/H_2O Al_2O_3. Finally, the use of two precursors (O_3 and H_2O) was shown to reduce C and H at the interface. On the other hand, it promotes a greater presence of undesired elements related to the etching and cleaning processes such as Cl and F.

ACKNOWLEDGEMENTS

The authors are grateful to M. Charles for the epitaxy, Patricia Pimenta Barros for the etching, E. Nguyen Gia Can for the ALD, and the CEA LETI process teams for samples fabrication. This work, carried out on the Platform for Nanocharacterization (PFNC), was supported by the "Recherches Technologiques de Base" program of the French National Research Agency (ANR). We also acknowledge the support of the Tandems collaboration project between PHI and Leti.

REFERENCES

[1] 'Futurs énergétiques 2050: les scénarios de mix de production à l'étude permettant d'atteindre la neutralité carbone à l'horizon 2050'. https://www.rte-france.com/analyses-tendances-et-prospectives/bilan-previsionnel-2050-futurs-energetiques

[2] F. Roccaforte *et al.*, 'Emerging trends in wide band gap semiconductors (SiC and GaN) technology for power devices', *Microelectron. Eng.*, vol. 187–188, pp. 66–77, Feb. 2018, doi: 10.1016/j.mee.2017.11.021.

[3] Guo, Haijun, et al., 'Breakdown mechanisms of power semiconductor devices.', *IETE Tech. Rev.*, 2018, doi: https://doi.org/10.1080/02564602.2018.1450652.
[4] G. Meneghesso, M. Meneghini, and E. Zanoni, Eds., *Power GaN Devices: Materials, Applications and Reliability*, 1st ed. 2017. Cham: Springer International Publishing : Imprint: Springer, 2017. doi: 10.1007/978-3-319-43199-4.
[5] R. Quay, *Gallium Nitride Electronics*, 96 vols. 2008 ISBN: 978-3-540-71890-1
[6] A. Lidow, J. Strydom, M. D. Rooij, and D. Reusch, *GaN Transistors for Efficient Power Conversion* ISBN: 9781119594147
[7] H. et.al Jiaqi, 'Recent Advances in GaN-Based Power HEMT Devices', 2021, doi: https://doi.org/10.1002/aelm.202001045.
[8] C. Le Royer *et al.*, 'Normally-OFF 650V GaN-on-Si MOSc-HEMT Transistor: Benefits of the Fully Recessed Gate Architecture', in *2022 IEEE 34th International Symposium on Power Semiconductor Devices and ICs (ISPSD)*, Vancouver, BC, Canada, May 2022, pp. 49–52. doi: 10.1109/ISPSD49238.2022.9813672.
[9] E. Brianna S., 'Electronic surface and dielectric interface states on GaN and AlGaN', *J. Vac. Sci. Technol. A*, 2013, doi: https://doi.org/10.1116/1.4807904.
[10] T. Hossain, 'Effect of GaN surface treatment on Al2O3/n-GaN MOS capacitors', *J. Vac. Sci. Technol. B*, 2015, doi: https://doi.org/10.1116/1.4931793.
[11] L. Vauche *et al.*, 'Study of an Al_2O_3 /GaN Interface for Normally Off MOS-Channel High-Electron-Mobility Transistors Using XPS Characterization: The Impact of Wet Surface Treatment on Threshold Voltage V_{TH}', *ACS Appl. Electron. Mater.*, vol. 3, no. 3, pp. 1170–1177, Mar. 2021, doi: 10.1021/acsaelm.0c01023.
[12] R. Caroline, 'Impact of surface treatments on high-κ dielectric integration with Ga-polar and N-polar GaN', *J. Vac. Sci. Technol. B*, 2014, doi: https://doi.org/10.1116/1.4831875.
[13] S. Tanuma, C. J. Powell, and D. R. Penn, 'Calculations of electron inelastic mean free paths. IX. Data for 41 elemental solids over the 50 eV to 30 keV range', *Surf. Interface Anal.*, vol. 43, no. 3, pp. 689–713, Mar. 2011, doi: 10.1002/sia.3522.
[14] K. Takhar, B. B. Upadhyay, Y. K. Yadav, S. Ganguly, and D. Saha, 'Al2O3 formed by post plasma oxidation of Al as a Gate dielectric for AlGaN/GaN MIS-HEMTs', *Appl. Surf. Sci.*, vol. 481, pp. 219–225, Jul. 2019, doi: 10.1016/j.apsusc.2019.03.065.
[15] M. C. S. Escaño *et al.*, 'On the presence of Ga2O sub-oxide in high-pressure water vapor annealed AlGaN surface by combined XPS and first-principles methods', *Appl. Surf. Sci.*, vol. 481, pp. 1120–1126, Jul. 2019, doi: 10.1016/j.apsusc.2019.03.196.
[16] K. Kim and J. Jang, 'Polarization-Charge Inversion at Al2O3/GaN Interfaces through Post-Deposition Annealing', *Electronics*, vol. 9, no. 7, p. 1068, Jun. 2020, doi: 10.3390/electronics9071068.
[17] Y. Gao, 'A new secondary ion mass spectrometry technique for III-V semiconductor compounds using the molecular ions CsM^+', *J. Appl. Phys.*, vol. 64, no. 7, pp. 3760–3762, Oct. 1988, doi: 10.1063/1.341381.
[18] C. Hongo, M. Tomita, and M. Suzuki, 'Quantitative secondary ion mass spectrometry analysis of impurities in GaN and Al xGa1yx N films using molecular ions MCsq and MCsq2', p. 4, 1999, doi: https://doi.org/10.1016/S0169-4332(98)00815-0.
[19] B. Saha and P. Chakraborty, 'MCsn+-SIMS: An Innovative Approach for Direct Compositional Analysis of Materials without Standards', *Energy Procedia*, vol. 41, pp. 80–109, 2013, doi: 10.1016/j.egypro.2013.09.009.
[20] S. Huang *et al.*, 'High-temperature low-damage gate recess technique and ozone-assisted ALD-grown Al2O3 gate dielectric for high-performance normally-off GaN MIS-HEMTs', in *2014 IEEE International Electron Devices Meeting*, San Francisco, CA, USA, Dec. 2014, p. 17.4.1-17.4.4. doi: 10.1109/IEDM.2014.7047071.
[21] Z. Shen, H. Liang, and et. al, 'Investigation of O3-Al2O3/H2O-Al2O3 dielectric bilayer deposited by atomic-layer deposition for GaN MOS capacitors', doi: 10.1002/pssa.201532785.

[22] T. Kubo, J. J. Freedsman, Y. Iwata, and T. Egawa, 'Electrical properties of GaN-based metal–insulator–semiconductor structures with Al_2O_3 deposited by atomic layer deposition using water and ozone as the oxygen precursors', *Semicond. Sci. Technol.*, vol. 29, no. 4, p. 045004, Apr. 2014, doi: 10.1088/0268-1242/29/4/045004.
[23] J. B. Kim, D. R. Kwon, K. Chakrabarti, C. Lee, K. Y. Oh, and J. H. Lee, 'Improvement in Al2O3 dielectric behavior by using ozone as an oxidant for the atomic layer deposition technique', *J. Appl. Phys.*, vol. 92, no. 11, pp. 6739–6742, Dec. 2002, doi: 10.1063/1.1515951.
[24] S. Jakschik *et al.*, 'Physical characterization of thin ALD–Al2O3 films', *Appl. Surf. Sci.*, vol. 211, no. 1–4, pp. 352–359, Apr. 2003, doi: 10.1016/S0169-4332(03)00264-2.